Randomly Diluted e_g Orbital-Ordered Systems

T. Tanaka, M. Matsumoto,* and S. Ishihara

Department of Physics, Tohoku University, Sendai 980-8578, Japan

(Received 3 August 2005; published 21 December 2005)

Dilution effects on the long-range ordered state of the doubly degenerate e_g orbital are investigated. Quenched impurities without the orbital degree of freedom are introduced in the orbital model where the long-range order is realized by the order-from-disorder mechanism. It is shown by Monte Carlo simulations and the cluster-expansion method that a decrease in the orbital-ordering temperature by dilution is substantially larger than that in the randomly diluted spin models. Tilting of orbital pseudospins around impurities is the essence of this dilution effect. The present theory provides a new viewpoint for the recent resonant x-ray scattering experiments in $KCu_{1-x}Zn_xF_3$.

DOI: 10.1103/PhysRevLett.95.267204 PACS numbers: 75.30.−m, 71.10.−w, 71.23.−k, 78.70.−g

Impurity effects on the long-range ordered state are one of the attractive themes in a recent study of correlated electron systems [1]. A small amount of nonmagnetic impurities dramatically destroys the superconductivity in cuprates, and induces antiferromagnetic long-range order in the low-dimensional quantum spin liquids. Doped impurities also cause striking effects on the charge and orbital orders; substitution of Cr ions for Mn in colossal magnetoresistive (CMR) manganites immediately destroys the charge-orbital orders [2]. The origin of CMR itself is studied from the viewpoint of randomness and/or percolation [3].

Recently, the dilution effects in $KCuF_3$ by substituting Zn for Cu have been reported experimentally by Tatami *et al.* [4]. A Cu^{2+} ion in the cubic-crystalline field shows the $t_{2g}^6 e_g^3$ configuration which has the e_g orbital degree of freedom. The Cu ions in the perovskite crystal form a 3D simple-cubic (SC) lattice and exhibit long-range orbital order (OO) at room temperatures, where the $d_{y^2-z^2}$- and $d_{z^2-x^2}$-like orbitals are aligned with momentum $\mathbf{Q} = (\pi, \pi, \pi)$. Since the five d orbitals are fully occupied in Zn^{2+}, substitution of Zn for Cu corresponds to dilution of the orbitals. The resonant x-ray scattering (RXS) studies in $KCu_{1-x}Zn_xF_3$ reveal that a decrease in the orbital-ordering temperature (T_{OO}) by dilution is much stronger than that in the randomly diluted magnets, and OO disappears around $x = 0.5$, as shown in the inset of Fig. 1. These observations may not be explained by the conventional percolation scenario; the site-percolation threshold in 3D SC lattice is $x_c(\equiv 1 - p_c) = 0.69$, which is well applicable to several diluted magnets, such as $KMn_{1-x}Mg_xF_3$ [5,6].

We examine, in this Letter, the dilution effects on the long-range order of the e_g orbital degree of freedom. As is well known, the doubly degenerate e_g orbital is treated by the pseudospin (PS) operator with a magnitude of 1/2; $\mathbf{T}_i = \frac{1}{2}\sum_{\gamma,\gamma',s} d^\dagger_{i\gamma s}\sigma_{\gamma\gamma'}d_{i\gamma' s}$, where $d_{i\gamma s}$ indicates the annihilation operator of a hole with spin s and orbital γ at site i and σ are the Pauli matrices. The shape of the electronic orbital is described by an angle θ of the PS vector as $|\theta\rangle = \cos(\theta/2)|d_{3z^2-r^2}\rangle + \sin(\theta/2)|d_{x^2-y^2}\rangle$. For example, $\theta = 0$, $2\pi/3$, and $4\pi/3$ correspond to the $d_{3z^2-r^2}$, $d_{3y^2-r^2}$, and $d_{3x^2-r^2}$ orbitals, respectively, and $\theta = \pi, 5\pi/3$, and $\pi/3$ to $d_{x^2-y^2}$, $d_{z^2-x^2}$, and $d_{y^2-z^2}$, respectively. As shown below, the Hamiltonian for the diluted orbital system is described by the PS operators and seems to be on the same footing with the spin models. However, the obtained results are qualitatively different from the diluted magnets. The main results are shown in Fig. 1. The impurity-concentration x dependences of T_{OO}, calculated by two different methods, namely, the numerical Monte Carlo (MC) method and the analytical cluster-expansion (CE) method, show rapid decreases in comparison with that in the spin models. By applying the present theory, $KCu_{1-x}Zn_xF_3$ [4] is interpreted to be a nice example of the unusual dilution effect in the e_g orbital system.

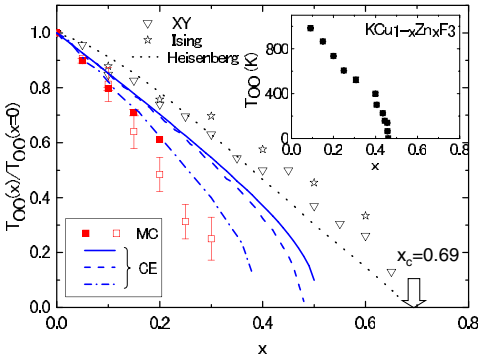

FIG. 1 (color online). Impurity-concentration dependence of the normalized orbital-ordering temperature $T_{OO}(x)/T_{OO}(x = 0)$. The calculated results by the MC method are shown by the solid and open red squares (see text), and those by the CE method for the one- and two-site clusters are shown by the solid and dashed lines, respectively. The results by the CE method where the PS operator is treated as a classical vector are shown by the one-point chain line. For comparison, T_N in the XY (down-pointing triangles) and Ising (stars) models by the MC method, and that in the Heisenberg model (dotted line) by the CE method, are also shown. The inset shows the Zn concentration dependence of T_{OO} in $KCu_{1-x}Zn_xF_3$ obtained by the RXS experiments [4].

The model Hamiltonian adopted here describes the orbital interaction between the nearest-neighbor (NN) Cu sites in a 3D SC lattice:

$$\mathcal{H} = 2J\sum_{\langle ij\rangle}\tau_i^l\tau_j^l\varepsilon_i\varepsilon_j, \quad (1)$$

where $J(>0)$ is the interaction and $\langle ij\rangle$ indicates a pair of the NN sites along the direction $l(= x, y, z)$. The operator τ_i^l depends explicitly on the bond direction and is defined by a linear combination of the PS operators as

$$\tau_i^l = \cos\left(\frac{2\pi}{3}n_l\right)T_{iz} - \sin\left(\frac{2\pi}{3}n_l\right)T_{ix}, \quad (2)$$

with $(n_x, n_y, n_z) = (1, 2, 3)$. The quenched impurities without the orbital degree of freedom are introduced by ε_i taking one and zero for Cu and Zn, respectively.

The Hamiltonian in Eq. (1) without impurities ($\varepsilon_i = 1$ for $\forall i$) has two different physical origins of the interaction, i.e., the electronic and/or phononic interactions. In the electronic viewpoint, this is derived by the generalized-Hubbard model with the e_g orbital degree of freedom. Through the perturbational expansion with respect to the NN electron transfer t, the spin-orbital superexchange model is obtained [7,8]; $\mathcal{H}_{\rm ST} = -2J_1\sum_{\langle ij\rangle}(\frac{3}{4} + \mathbf{S}_i\cdot\mathbf{S}_j)\times(\frac{1}{4} - \tau_i^l\tau_j^l) - 2J_2\sum_{\langle ij\rangle}(\frac{1}{4} - \mathbf{S}_i\cdot\mathbf{S}_j)(\frac{3}{4} + \tau_i^l\tau_j^l + \tau_i^l + \tau_j^l)$. Here, $\mathbf{S}_i$ is the spin operator at site i with a magnitude of $1/2$, and J_1 [$= t^2/(U - 3I)$] and J_2 ($= t^2/U$) are the superexchange interactions with the on-site intraorbital Coulomb interaction U and the exchange interaction I. Since the Néel temperature ($T_{\rm N}$) in $KCu_{1-x}Zn_xF_3$ is far below $T_{\rm OO}$ in a whole range of x [4], taking $\mathbf{S}_i\cdot\mathbf{S}_j = 0$ is a good assumption, and Eq. (1) with $J = \frac{3}{4}J_1 - \frac{1}{4}J_2$ is obtained. In the phononic viewpoint, the orbital model is derived based on the cooperative Jahn-Teller (JT) effects. Start from the linear JT coupling Hamiltonian $\mathcal{H}_{\rm JT} = g\sum_{i,m=(x,z)}Q_{im}T_{im}$ with the vibrational modes Q_{im} ($m = x, z$) in a F_6 octahedron, and the lattice potential K between NN Cu-F bonds. After rewriting Q_{im} by the phonon coordinates $\mathbf{q}_\mathbf{k}$, we obtain Eq. (1) with $J = 2g^2/(9K)$ by integrating out $\mathbf{q}_\mathbf{k}$ [9,10]. The sign of J is positive in both processes. A unique aspect of the orbital model to be noticed here is that the explicit form of the interaction depends on the bond direction l; the interactions are $T_{iz}T_{jz}$ for $l = z$, and $[-\frac{1}{2}T_{iz} - (+)\frac{\sqrt{3}}{2}T_{ix}][-\frac{1}{2}T_{jz} - (+)\frac{\sqrt{3}}{2}T_{jx}]$ for $l = x(y)$. When we focus on one direction l, the staggered alignment of the $d_{3l^2-r^2}$ and $d_{m^2-n^2}$ orbitals with $(l, m, n) = (x, y, z), (y, z, x)$ and (z, x, y) is favored. In a 3D SC lattice with and without impurities, the stable orbital configurations are nontrivial.

We have attacked this issue by a numerical approach together with an analytical one, i.e., the classical MC simulation and the CE method. In the MC method, the PS operator is treated as a classical vector defined in the $T_x - T_z$ plane. The MC calculations have been performed for the cubic $L\times L\times L$ lattice ($L = 10\sim 18$) with the periodic-boundary condition. For each sample, 30 000 MC steps are spent for measurement after 8000 MC steps for thermalization. The physical quantities are averaged over 20–80 MC samples at each parameter set. We adopt the CE method proposed in Ref. [11], where the fluctuations of the effective fields are self-consistently determined with the order parameter. Even in the two-site clusters, this CE method provides good values for x_c and the Curie temperature $T_{\rm C}$ at $x = 0$ for Ising and Heisenberg models [11].

First, we show the results without impurities. It is known that, in the orbital model [Eq. (1)] at $x = 0$, there is a macroscopic degeneracy in the mean-field (MF) ground state [12–16]. These are classified into two types: (i) One of the MF solutions is the staggered-type OO with two sublattices, termed A and B, and the momentum $\mathbf{Q} = (\pi, \pi, \pi)$. The orbital angles in the sublattices are $(\theta_A, \theta_B) = (\theta, \theta + \pi)$ for any value of θ. Such continuous-rotational symmetry is unexpected from Eq. (1). (ii) Consider an OO with $\mathbf{Q} = (\pi, \pi, \pi)$ and $(\theta_A, \theta_B) = (\theta_0, \theta_0 + \pi)$, and focus on one direction in a 3D SC lattice, e.g., the z direction. The MF energy is not changed by changing $(\theta_0, \theta_0 + \pi) \rightarrow (-\theta_0, -\theta_0 - \pi)$ in each layer in the xy plane. Both types of degeneracy are understood from the momentum representation of Eq. (1): $\mathcal{H} = \sum_\mathbf{k}\psi_\mathbf{k}^\dagger\hat{J}(\mathbf{k})\psi_\mathbf{k}$ with $\psi_\mathbf{k} = [T_{z\mathbf{k}}, T_{x\mathbf{k}}]$ and the 2×2 matrix $\hat{J}(\mathbf{k})$. By diagonalizing $\hat{J}(\mathbf{k})$, we obtain the eigenvalues $J_\pm(\mathbf{k}) = 2J[-c_x - c_y - c_z \pm \sqrt{c_x^2 + c_y^2 + c_z^2 - c_xc_y - c_yc_z - c_zc_x}]$ with $c_l = \cos(\pi k_l/a)$ [17]. $J_-(\mathbf{k})$ has its minimum along $(\pi, \pi, \pi) - (0, \pi, \pi)$ and other three-equivalent directions. A lifting of the degeneracy in the orbital model is discussed in Refs. [15,16] by spin-wave analyses. Here we show the lifting of the degeneracy by the MC method. In Fig. 2(a), the number of data obtained in the simulation is plotted as a function of the orbital angle θ in the staggered-type OO with $(\theta_A, \theta_B) = (\theta, \theta + \pi)$. It is shown that the type-(i) orbital degeneracy is lifted; θ is confined to the three discontinuous values of 0, $2\pi/3$, and $4\pi/3$. The inset

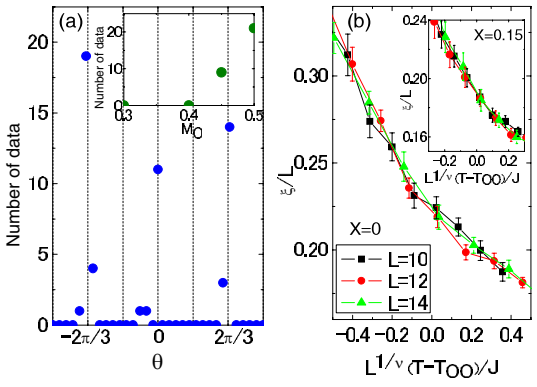

FIG. 2 (color online). (a) A MC data distribution for the orbital angle θ in the staggered-type orbital order at $x = 0$. The inset shows a data distribution of the order parameter $M_{\rm O}$ at $x = 0$. (b) The finite-size scaling for the correlation length ξ/L as functions of $L^{1/\nu}(T - T_{\rm OO})/J$ at $x = 0$. The inset shows the scaling plot at $x = 0.15$.

shows number of data as function of the orbital-order parameter M_O at $\mathbf{Q} = (\pi, \pi, \pi)$ defined as $M_O^2 = \sum_{m=x,z}\langle T_{\mathbf{Q}m} T_{-\mathbf{Q}m}\rangle$ with $T_{\mathbf{k}m} = \frac{1}{N}\sum_i e^{i\mathbf{k}\cdot\mathbf{r}_i} T_{im}$. Most of the data show $M_O = 0.5$, implying that the ordering pattern is of a staggered type, and the type-(ii) degeneracy is also lifted.

We have performed the finite-size scaling analyses in the MC simulation to determine T_{OO}. The correlation length ξ is calculated by the second-moment method in the PS correlation function for several sizes L. In Fig. 2(b), we demonstrate the scaling plot for ξ/L as a function of $(T - T_{OO})L^{1/\nu}$ at $x = 0$. The scaling analyses work quite well for $L = 10$, 12, and 14. T_{OO} and the exponent ν are determined through the least-square fitting by the polynomial expansion and obtained as $T_{OO}/J = 0.344 \pm 0.002$ and $\nu = 0.69$–0.81, although statistical errors are not enough to obtain the precise value of ν. Even in the diluted case [see the inset of Fig. 2(b)], the precision is enough to determine T_{OO} [$= (0.248 \pm 0.003)J$ for $x = 0.15$]. Beyond $x = 0.15$, the scaling analyses do not work well.

In Fig. 3(a), the temperature dependence of the normalized-order parameter $\frac{1}{1-x}M_O$ [$\equiv m_O(x, T)$] is presented. First, focus on the region of $x \leq 0.15$. As expected, $m_O(x = 0, T)$ abruptly increases at T_{OO} and is saturated to 0.5 at $T \to 0$. By doping impurity, $m_O(x, T)$ does not reach 0.5 even far below T_{OO}, and $m_O(x \neq 0, T \to 0)$ gradually decreases with increasing x. Although the system sizes are not sufficient to estimate $m_O(x, T)$ in the thermodynamic limit, $m_O(x \neq 0, T \to 0)$ does not show the smooth convergence to 0.5 in contrast to the diluted spin models. Beyond $x = 0.15$, the situation is changed qualitatively; in spite of the fact that $m_O(x, T)$ grows around a certain temperature (e.g., $\sim 0.18J$ at $x = 0.2$), $m_O(x, T \to 0)$ becomes small abruptly and decreases weakly with increasing L. Anomalies in the specific heat and the susceptibility around this temperature become weak, and some of the

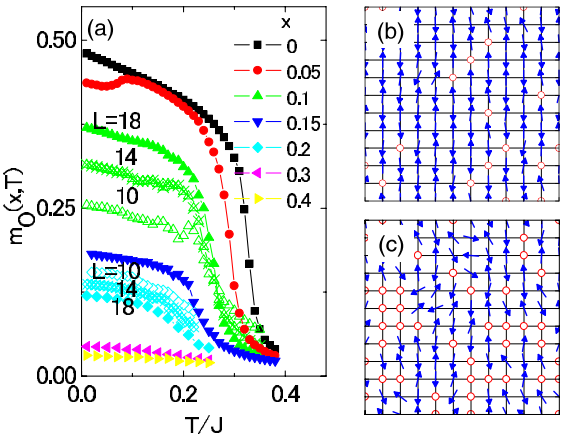

FIG. 3 (color online). (a) Temperature dependence of the normalized-order parameter $m_O(x, T)$ [$= M_O/(1 - x)$] for various x and L. (b) A snapshot in the MC simulation for the PS configuration at $x = 0.1$. Open circles indicate the impurities. (c) A snapshot at $x = 0.3$.

physical quantities, e.g., $N_O \equiv \sum_{m=x,z}\langle T_{\mathbf{Q}m}\rangle^2$ with $\mathbf{Q} = (\pi, \pi, \pi)$, depend on the initial states in the MC simulation. It seems that the orbital correlation grows below this temperature, but the long-range order does not. We suppose that a possible orbital state in this region is a short-range ordered state or a glass state [18], although unclear at the present stage. Thus, in $x > 0.15$, a temperature where $dm_O(x, T)/dT$ in $L = 18$ takes a maximum is interpreted to be the crossover and/or glass-transition temperature. Above $x = 0.3$, estimation of T_{OO} becomes severe because of the weak temperature dependence of $m_O(x, T)$. Thus, as supplementary information of the ordering temperature, we calculate a temperature $\tilde{T}_{OO}$ where dN_O/dT takes a maximum, and consider its full width at half maximum as an error. The initial state in the calculation for $\tilde{T}_{OO}$ is assumed to be the ordered state, although the initial-state dependence of $\tilde{T}_{OO}$ is much weaker than that of the N_O amplitude.

The x dependences of T_{OO} presented in Fig. 1 are obtained by the MC (solid red squares) and CE (blue lines) methods introduced above. $\tilde{T}_{OO}$'s by the MC method are also shown by the open red squares. For comparison, the x dependences of T_N in the spin models are plotted. Starting to dope impurities in the orbital model, decrease of T_{OO} is much stronger than that of T_N in the spin models. Around $x = 0.15$, the clear transition to the long-range order becomes obscure, explained above. $\tilde{T}_{OO}$'s obtained by N_O are close to T_{OO} below $x = 0.2$, and decrease smoothly up to $x = 0.3$, although the critical x, where $\tilde{T}_{OO}$ disappears, is not determined due to large statistical errors. A rapid decrease of T_{OO} is also obtained by the CE method. It is seen that the difference between the calculated $T_{OO} - x$ curves for the cluster sizes $N_C = 1$ (solid line) and 2 (dashed line) is within a few percent. T_{OO} in the CE method disappears around $x = 0.5$ being much smaller than $x_c = 0.69$ for the 3D SC lattice. We also calculate T_{OO} in the CE method where the quantum PS operators are replaced by the classical vectors. The calculated results plotted by the one-point chain line are close qualitatively to the $T_{OO}(\tilde{T}_{OO}) - x$ curve obtained by the classical MC method.

Now we introduce the physical picture of the diluted orbital-ordered state. The real-space configurations of the orbital PSs help us to understand the calculated $T_{OO} - x$ curve. The MC snapshots of the PSs on a plane are shown in Figs. 3(b) and 3(c) for $x = 0.1$ and 0.3, respectively. The staggered-type OO with the orbital angles $(\theta_A, \theta_B) = (0, \pi)$ is seen in the background of Fig. 3(b). At the neighboring sites of the impurities indicated by the open circles, tiltings of the PS vectors are observed. Disturbing the PS configuration from $(0, \pi)$ becomes violent at $x = 0.3$. These observations are caused by the local-symmetry breaking by dilution. Consider the orbital state at a neighboring site of an impurity on the x axis. On account of the impurity, one of the interactions along x vanishes. Since the interaction depends on the bond direction explicitly in the orbital model, the PS at this site tilts to gain the

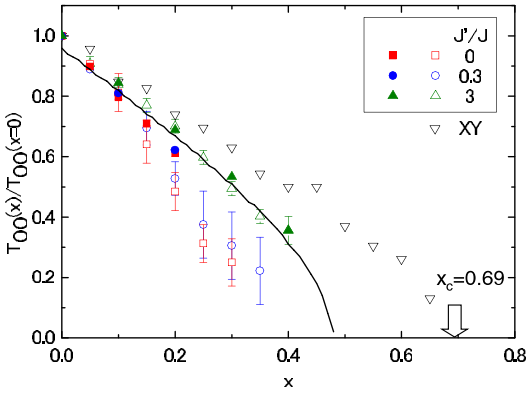

FIG. 4 (color online). Impurity-concentration dependence of the normalized orbital-ordering temperature $T_{\mathrm{OO}}(x)/T_{\mathrm{OO}}(x=0)$ with the higher-order JT coupling. The squares, circles, and triangles indicate $T_{\mathrm{OO}}(x)/T_{\mathrm{OO}}(x=0)$ at $J'/J=0$, 0.3, and 3, respectively. T_{OO}'s indicated by the open and solid symbols are defined in the text. For comparison, T_{N} of the XY model (down-pointing triangles) and T_{OO} at $J'/J=0$ by the CE method (solid line) are also plotted.

interaction energies for other five bonds. This is the essence of the diluted orbital systems and is in contrast to the conventional diluted spin models. To check roles of this PS tilting on the anomalous $T_{\mathrm{OO}}-x$ curve, we have performed the MC calculations in the model where the available orbital angles in the T_z-T_x plane are restricted to a few states. The obtained $T_{\mathrm{OO}}-x$ curve is similar to that in the spin models; the tilting of PSs is confirmed to be the origin of the rapid decrease of T_{OO}.

Finally, to more directly compare the present theory with the experiments in $KCu_{1-x}Zn_xF_3$, we introduce the higher-order JT coupling. From the RXS experiments [4] and the lattice distortion in $KCuF_3$ [19], the OO in $KCuF_3$ is expected to be the $d_{y^2-z^2}/d_{z^2-x^2}$ type: the cant-type OO with the orbital angles $(\theta,-\theta)$ $(\theta\sim\pi/3)$ and $\mathbf{Q}=(\pi,\pi,\pi)$. To reproduce this type of OO, the higher-order JT coupling is required, $\mathcal{H}_{\mathrm{HJT}}=g'\sum_i\{(Q_{iz}^2-Q_{ix}^2)T_{iz}-2Q_{iz}Q_{ix}T_{ix}\}$, which provides the anisotropy in the PS space. Here we treat approximately this term based on the theory of the cooperative JT effects. By rewriting $Q_{ix(z)}$ by the phonon coordinates $\mathbf{q_k}$, and by integrating out $\mathbf{q_k}$, the interaction between orbitals at the different three-neighboring sites is obtained: $\mathcal{H}'=J'\sum_{\langle ijk\rangle}\{(T_{iz}T_{jz}+T_{ix}T_{jx})T_{kz}-2T_{iz}T_{jx}T_{kx}\}\varepsilon_i\varepsilon_j\varepsilon_k$. Here, $J'=(16g'g^2)/(9K^2)$ is the coupling constant and $\langle ijk\rangle$ indicates a sum of the neighboring three sites. The MF energy of $\mathcal{H}'$ is proportional to $\frac{J'}{8}\times\cos3\theta$, implying anisotropy. A value of g' for a Cu^{2+} ion was estimated by the adiabatic potential barrier in a molecule [20] and corresponds to J' being about $0.3J$. We have performed the MC calculations in the model of $\mathcal{H}+\mathcal{H}'$ and observed that the cant-type OO at $x=0$ is realized. The doping dependences of T_{OO} (and $\tilde{T}_{\mathrm{OO}}$), including $\mathcal{H}'$, are presented in Fig. 4 for $J'/J=0.3$ and 3. The solid and open symbols are for T_{OO} and $\tilde{T}_{\mathrm{OO}}$, respectively, which are obtained by the same ways with those in Fig. 1. With an increase in J', the $T_{\mathrm{OO}}(\tilde{T}_{\mathrm{OO}})-x$ curves approach those for the spin models, because the anisotropy suppresses the tilting of PSs. However, we confirm that the rapid reduction of T_{OO} by dilution survives even in the calculation with the realistic value of J', and is consistent with the RXS experimental results shown in the inset of Fig. 1.

In summary, we have investigated the dilution effects on the long-range order of the e_g orbital degree of freedom. We confirm, by both MC and CE methods, that T_{OO} decreases rapidly with doping, in comparison with the diluted magnets. The tilting of the orbital PSs around impurities, which is distinguished qualitatively from the spin models, is the essence for the rapid decrease of T_{OO}. The rapid reduction of T_{OO} experimentally observed in $KCu_{1-x}Zn_xF_3$ [4] is explained by the present unique dilution effects in the e_g orbital systems. A broad peak profile observed by the RXS experiments [4] may be attributed to the orbital tilting around impurities. Observations of the tilting by the scanning-tunneling microscope and/or the scanning-electron microscope are a direct check for the present results.

The authors would like to thank Y. Murakami for valuable discussions and permission to use the experimental data before publication. This work was supported by KAKENHI from MEXT, NAREGI, and CREST. Part of the numerical calculation was performed by the supercomputers in IMR, Tohoku University, and ISSP, University of Tokyo. T. T. appreciates financial support from JSPS. M. M. thanks S. Todo for helpful discussions.

*Present address: Institute for Theoretical Physics, ETH-Hönggerberg, CH-8093 Zürich, Switzerland.

[1] S. Maekawa *et al.*, *Physics of Transition Metal Oxides* (Springer Verlag, Berlin, 2004), and references therein.
[2] A. Barnabe *et al.*, Appl. Phys. Lett. **71**, 3907 (1997).
[3] M. Uehara *et al.*, Nature (London) **399**, 560 (1999).
[4] N. Tatami, S. Niioka, and Y. Murakami (to be published); N. Tatami, Master thesis, Tohoku University, 2004.
[5] R. B. Stinchcombe, in *Phase Transition in Critical Phenomena*, edited by C. Domb and J. L. Lebowitz (Academic Press, London, 1983), Vol. 7.
[6] D. J. Breed *et al.*, J. Appl. Phys. **41**, 1267 (1970).
[7] K. I. Kugel *et al.*, Sov. Phys. JETP **37**, 725 (1973).
[8] S. Ishihara *et al.*, Phys. Rev. B **55**, 8280 (1997).
[9] J. Kanamori, J. Appl. Phys. **31**, S14 (1960).
[10] S. Okamoto *et al.*, Phys. Rev. B **65**, 144403 (2002).
[11] H. Mano, Prog. Theor. Phys. **57**, 1848 (1977).
[12] L. F. Feiner *et al.*, Phys. Rev. Lett. **78**, 2799 (1997).
[13] G. Khaliullin *et al.*, Phys. Rev. B **56**, R14243 (1997).
[14] S. Ishihara *et al.*, Phys. Rev. B **62**, 2338 (2000).
[15] K. Kubo, J. Phys. Soc. Jpn. **71**, 1308 (2002).
[16] Z. Nussinov *et al.*, Europhys. Lett. **67**, 990 (2004).
[17] S. Ishihara *et al.*, Phys. Rev. B **56**, 686 (1997).
[18] K. Binder *et al.*, Adv. Phys. **41**, 547 (1992).
[19] K. Hirakawa *et al.*, Prog. Theor. Phys. Suppl. **46**, 147 (1970).
[20] S. Shashkin *et al.*, Phys. Rev. B **33**, 1353 (1986).